

Establishment and characterization of endometrial organoids from different placental types

Dong-Hyeok Kwon^{1,2,3,#}, Byeonghwi Lim^{4,#}, Sung-Yeon Lee^{1,#}, Sung-Ho Won⁵ & Goo Jang^{1,2,3,*}

¹Laboratory of Theriogenology, College of Veterinary Medicine, Seoul National University, Seoul 08826, ²BK21 FOUR Future Veterinary Medicine Leading Education and Research Center, Seoul National University, Seoul 08826, ³Comparative Medicine Disease Research Center, Seoul National University, Seoul 08826, ⁴Department of Animal Science and Technology, Chung-Ang University, Anseong 17546,

⁵Department of Public Health Sciences, Institute of Health & Environment, School of Public Health, Seoul National University, Seoul 08826, Korea

Understanding molecular characteristics and metabolic processes of the mammalian endometrium is crucial for advancing biological research, particularly in veterinary obstetrics and pathology. This study established and analyzed organoids from endometrial epithelial stem cells of five mammals with different placental types: cows (cotyledonary), dogs and cats (zonary), pigs (diffuse), and rats (discoid). Organoids from these five species were maintained for over 13 passages, frozen, and thawed. Pathological analysis confirmed that they retained characteristics of their original tissues. Furthermore, integrative transcriptome analysis of organoids and tissues from the five species highlighted key pathways such as PI3K-Akt signaling and extracellular matrix-receptor interaction known to be crucial in cancer research. Although genes associated with vascular smooth muscle contraction were downregulated, these organoids exhibited significant activities of genes involved in hormone metabolism. In conclusion, our study achieved stable establishment of endometrial organoids from five mammals with different placental types, offering foundational data for organoid research. In the future, these organoids are suitable models for investigating uterine physiology and diseases and for developing potential therapies. [BMB Reports 2025; 58(2): 95-103]

INTRODUCTION

Investigating molecular characteristics and biological metabolic processes of the mammalian endometrium plays a crucial role in modern medicine, facilitating a comprehensive understanding

of obstetric pathology (1, 2). During pregnancy, the endometrium nourishes the placenta and changes cyclically in response to steroid hormones such as estrogen and progesterone (3). Unlike humans and some primates, most mammals do not experience menstruation, which involves periodic thickening and shedding of the endometrium. Instead, these animals undergo estrous cycles, where the endometrium changes in preparation for pregnancy and, if implantation does not occur, it is reabsorbed or partially expelled (4). These cyclical changes are crucial for preparing the endometrium for pregnancy and supporting embryo implantation and maintenance. Consequently, the mammalian endometrium plays a vital role in embryo implantation and pregnancy maintenance by expressing metabolism-related genes that can maintain energy balance (5, 6).

However, research on the endometrium presents significant challenges due to difficulty of accessing uterus and ethical constraints associated with obtaining tissues through invasive surgical procedures (7, 8). Furthermore, although *in vitro* studies such as primary cell cultures can complement *in vivo* investigations, they are hindered by difficulties of sustaining *in vitro* culturing. In addition, they might yield discordant outcomes compared to *in vivo* organ systems (9). To overcome these limitations, endometrial organoids present an innovative solution, offering an ethical and applicable methodology for studying the endometrial epithelium. Organoids are self-assembling, three-dimensional (3D) *in vitro* culture models derived from epithelial stem cells that are considered promising alternatives to *in vivo* models (10). They can effectively replicate the physiology of their source organs or tissues, including genetic diversity, various cell types, and a significant portion of their functionality. Thus, organoids provide a more efficient and cost-effective solution for cellular physiology, disease modeling, drug development including drug screening and repurposing, and personalized medicine than animal experiments (11, 12). Moreover, these endometrial organoids provide a more accurate model system than traditional two-dimensional (2D) cell cultures by replicating the complex 3D structure of endometrial epithelial cells (13).

Despite the promise of organoids, contemporary endometrial research has primarily focused on humans and mice that possess

*Corresponding author. Tel: +82-2-880-1280; Fax: +82-2-880-8662;
E-mail: snujang@snu.ac.kr

#These authors contributed equally to this work.

<https://doi.org/10.5483/BMBRep.2024-0141>

Received 10 September 2024, Revised 29 October 2024,
Accepted 15 December 2024, Published online 22 January 2025

Keywords: Endometrium, Mammals, Organoids, Placenta, Transcriptome, Uterus

discoid placentas, leading to a lack of studies on mammals with different placental types (3, 14). This gap highlights several limitations in endometrial research within veterinary obstetrics. Therefore, this study mainly addresses shortcomings of existing research by establishing stable models of endometrial organoids from five mammals with unique placental types: cotyledonary in cows, zonary in dogs and cats, diffuse in pigs, and discoid in rats (15). These species were selected as representatives of their respective placental types, with each exhibiting unique structural and functional characteristics that could offer comprehensive insights into the diversity of endometrial biology. By isolating and culturing organoids from epithelial stem cells of endometria of these species, we aimed to establish foundational data for endometrial organoid research in veterinary science.

Herein, we used RNA sequencing (RNA-seq) to analyze transcriptomes of 3D organoids isolated from endometria of five mammals and cultured *in vitro* by comparing them to *in vivo* transcriptomes of these endometria. This study enabled us to evaluate characteristics of endometrial organoids from each species and define their molecular roles. By establishing these diverse endometrial organoids and generating comprehensive transcriptomic data, this study provides crucial foundational data for uterine disease models, regenerative medicine, and drug development. Ultimately, it serves as a cornerstone for future studies in veterinary obstetrics, addressing ethical issues associated with the use of experimental animals. In addition, it attempts to enhance the overall quality and practicality of endometrial organoid research by discussing obstacles faced by current methodologies.

RESULTS

Establishment of endometrial organoids from five mammals
Uterine samples, each measuring 3 cm in length, were collected from each species. These samples were divided into three equal parts: one-third for organoid culture, one-third for total RNA extraction, and the remaining for fixation in 4% paraformaldehyde (PFA) (Fig. 1A). Each species' endometrial organoid was passaged every 7 days: 19 passages for cow (bovine), 13 passages for dog (canine), cat (feline), and pig (porcine), and 30 passages for rat (rattus). All organoids exhibited robust proliferation, maintaining consistent sizes and proliferation rates for each individual species throughout their long-term culture. Diameters of organoids varied among species, with rat showing the largest mean diameter ($217.23 \pm 82.92 \mu\text{m}$), followed by pig ($159.20 \pm 65.87 \mu\text{m}$), dog ($81.38 \pm 22.20 \mu\text{m}$), cat ($58.04 \pm 23.46 \mu\text{m}$), and cow ($50.71 \pm 16.57 \mu\text{m}$) (Fig. 1B). Additionally, cryopreservation demonstrated that organoids from all species could be appropriately frozen, thawed, and subcultured for more than three passages (Supplementary Fig. 1).

Histological assessment

Similarities between uterine tissues and endometrial organoids from the five mammals were analyzed using histological staining and immunohistochemistry (IHC) to validate their resemblance in structure and function. Hematoxylin and eosin (H&E) staining was utilized to assess general structural integrity. For organoids, H&E staining revealed organized glandular structures and cellular arrangement that closely mirrored morphologies of their original endometrial tissues, confirming their structural similarities. Periodic Acid-Schiff (PAS) staining for detecting

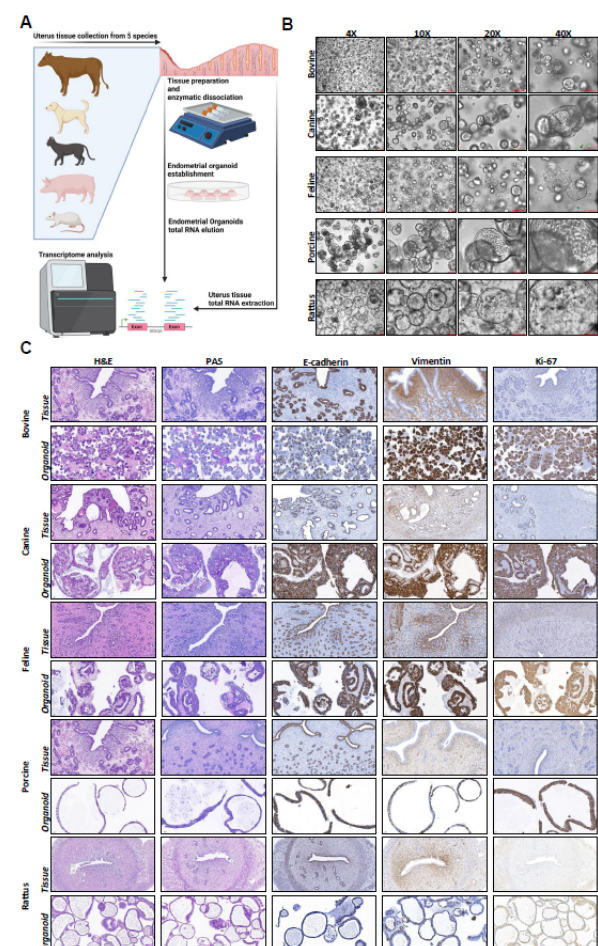


Fig. 1. Establishment of organoid and histological analyses. (A) Schematic representation of the experimental design. Uterine samples from five mammals (cow, dog, cat, pig, and rat) were divided into three parts: one-third for organoid culture, one-third for RNA extraction, and one-third for immunohistochemistry (IHC). (B) Endometrial organoids from five mammalian species were cultured and passaged over 13 times. Representative images at $\times 4$, $\times 10$, $\times 20$, and $\times 40$ magnifications are shown. All organoids were imaged on day 7 of culture after more than 13 passages. The scale bar indicate $100 \mu\text{m}$ ($\times 4$, $\times 10$, and $\times 20$) or $50 \mu\text{m}$ ($\times 40$). (C) Comparisons of endometrial organoids and endometria of five mammals. Histological staining (Hematoxylin-Eosin [H&E] and Periodic Acid-Schiff [PAS] stain) and IHC (E-cadherin, vimentin, and Ki-67) demonstrate similarity between endometrial organoids and tissues.

glycogen identified polysaccharides within organoids. This was indicative of mucinous cell activity similar to that of endometrial glands, suggesting that these organoids possessed functional aspects that could enable glycogen storage and secretion, a key glandular function. For IHC, E-cadherin, a cell adhesion molecule prominently expressed in epithelial cells, was used to assess epithelial alignment and tissue integrity. E-cadherin was found to be expressed in organoids, validating the preservation of glandular epithelial characteristics akin to their original tissues and ensuring their structural integrity and epithelial arrangement similar to those of endometria. Vimentin, an intermediate filament protein associated with mesenchymal cells, highlighted mesenchymal–epithelial transition within organoids, suggesting a structural adaptability that included both stromal and epithelial components akin to the original tissue environment. Ki-67, a nuclear protein associated with cellular proliferation, exhibited high expression levels within organoids, indicating active cell division. This proliferation marker underscored the capacity of these organoids to replicate regenerative processes of endometrial tissues observed in the menstrual cycle (Fig. 1C).

Transcriptome profiling

A total of 343,147,830 trimmed reads were obtained from organoids and tissues of the five species, with an average of 34,314,783 reads per sample. The average mapping rate was 98.50%. Raw reads and mapping rates for samples are summarized in Supplementary Table 1. Using mapped data, we identified differentially expressed genes (DEGs) in comparison with tissues for each species (Supplementary Fig. 2; Supplementary Table 2). Subsequently, we compared all endometrial organoids ($n = 5$) and all endometrial tissues ($n = 5$) isolated from each species to investigate unique characteristics of these organoids relative to tissues. Compared to tissues, 707 DEGs were identified in organoids, with 155 DEGs being upregulated and 452 DEGs being downregulated (Fig. 2A; Supplementary Table 3). Functional analysis based on Gene Ontology (GO) terms was sorted with criteria of P-value < 0.05 and count ≥ 3 . In biological processes (BPs), “GO: 0050731 positive regulation of peptidyl-tyrosine phosphorylation” and “GO: 0001525 angiogenesis” were identified. In cellular components (CCs), “GO: 0031012 extracellular matrix” was found. In molecular functions (MFs), “GO: 0005178 integrin binding” was predominant. These GO terms were integrated using the SimRel method based on the $-\log_{10}$ P-value (Fig. 2B; Supplementary Table 4). The Kyoto Encyclopedia of Genes and Genomes (KEGG)-based analysis with criteria of P-value < 0.05 and count ≥ 3 identified a total of 51 pathways, with “hsa04151: PI3K-Akt signaling pathway”, “hsa04512: ECM-receptor interaction”, and “hsa04510: focal adhesion” being the top three pathways. Notably, among the 51 identified pathways, “hsa00100: steroid biosynthesis” was the most functionally enriched one (Fig. 2C; Supplementary Table 5). Expression frequency differences using common genes across all samples are represented

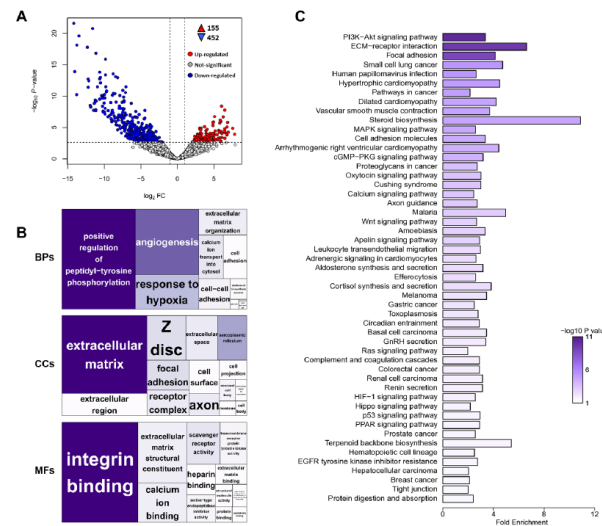


Fig. 2. Comprehensive transcriptome comparison of organoids versus tissues. (A) Volcano plot displaying differentially expressed genes (DEGs) in organoids by comparing all endometrial organoids ($n = 5$) and endometrial tissues ($n = 5$) isolated from each of the five species. All genes are annotated with human genes. There were 155 upregulated genes and 452 downregulated genes in organoids compared to tissues. The x-axis represents \log_2 fold-change (FC) and the y-axis represents $-\log_{10}$ P-value. (B) Gene Ontology (GO)-based functional enrichment of identified DEGs represented as a tree map of biological processes (BPs), cellular components (CCs), and molecular functions (MFs). (C) Kyoto Encyclopedia of Genes and Genomes (KEGG)-based functional enrichment analysis identified a total of 51 pathways. Each pathway's significance is indicated by $-\log_{10}$ P-value and fold enrichment value. All GO and KEGG terms adhered to the threshold criteria of P-value < 0.05 and count ≥ 3 .

using multidimensional scaling (MDS) (Supplementary Fig. 3).

Integrated network and clustering

To identify unique characteristics of each organoid and tissue, we performed a gene co-expression network (GCN) and K-means clustering analysis using the list of 707 DEGs identified in organoids. Consequently, the network generated a total of 1,460 nodes (genes) and 7,274 edges (interactions) (Fig. 3A). For clustering, 113 organoid-specific genes and 247 tissue-specific genes were identified. By species, we found 68 organoid-specific and 95 tissue-specific genes in bovine, 66 organoid-specific and 86 tissue-specific genes in canine, 52 organoid-specific and 97 tissue-specific genes in feline, 64 organoid-specific and 157 tissue-specific genes in porcine, and 54 organoid-specific and 103 tissue-specific genes in ratus (Fig. 3B). Supplementary Table 6 summarizes a detailed list of these genes and Supplementary Fig. 4 displays six clusters not specifically identified in any samples. KEGG-based functional analysis of the organoid-specific cluster (Cluster 7) revealed that pathways related to hormone metabolism, such as “hsa00100: steroid biosynthesis”, were the most significantly enriched pathways

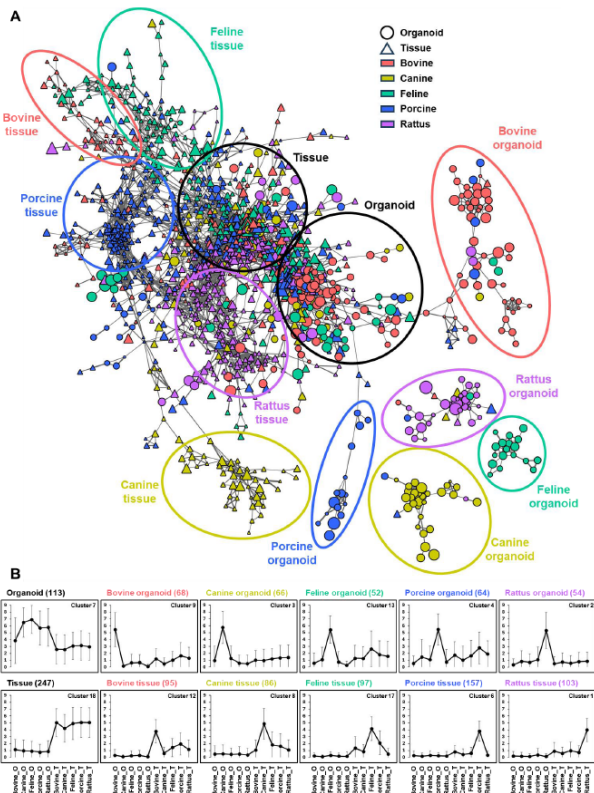


Fig. 3. Comprehensive expression network and cluster analysis of organoid and tissue differentially expressed genes (DEGs). (A) A co-expression network based on DEGs identified in five types of organoids and tissues, showing expression specificity of each type and sample. Each circle included in the network visualization indicates clusters specifically identified in each sample. The legend is displayed in the top-right corner. (B) Number of genes specifically expressed in each sample among 18 K-means clusters is shown. Columns labeled as “O” indicate organoid-specific clusters and those labeled as “T” indicate tissue-specific clusters.

(P-value = 1.48E-07) (Supplementary Table 7). In contrast, tissue-specific clusters (Cluster 18) showed that “hsa04270: vascular smooth muscle contraction” was the most significantly enriched pathway (P-value = 5.29E-09) (Supplementary Table 8).

Compilation of a specific pathway gene list

We examined whether the steroid biosynthesis pathway identified in the organoid-specific cluster (Cluster 7) and the vascular smooth muscle contraction pathway identified in the tissue-specific cluster (Cluster 18) were common pathways in other organoid clusters (Clusters 9, 3, 13, 4, and 2) and tissue clusters (Clusters 12, 8, 17, 6, and 1) (Criteria: count \geq 3; P < 0.05). In the case of steroid biosynthesis, an additional but related pathway, hsa00140: steroid hormone biosynthesis (P = 1.8E-02), was identified in the porcine-specific cluster (Cluster 4) (Supplementary Table 7). By integrating these two path-

ways, we compiled a list of genes involved in “hormone metabolism” and compared them with DEGs identified across all species and organoid groups, ultimately securing a common list of 24 genes. A heatmap (Supplementary Fig. 5A) was used to present expression patterns of these genes in each sample. Among the 24 genes, *HSD11B2* belonged to the tissue cluster (Cluster 18), *SQLE*, *DHCR7*, *CYP51A1*, *EBP*, *CYP3A7*, *TM7SF2*, and *CYP24A1* belonged to the organoid cluster (Cluster 7), and some genes were classified to specific organoid clusters (bovine: *SULT1E1*, canine: *CYP1A2*, porcine: *CYP2E1*, *CYP7A1*, and *UGT1A3*, and rattus: *HSD3B2*).

However, pathways similar to vascular smooth muscle contraction identified in the tissue cluster were not found in other clusters (Supplementary Table 8). A heatmap (Supplementary Fig. 5B) presented expression patterns of the 47 genes secured through comparison with DEGs in each sample. Among them, *ADM2* (organoid; Cluster 7), *ADCY2* (bovine organoid; Cluster 9), *CALCB* (feline organoid; Cluster 13), *MYH14* (porcine organoid; Cluster 4), and *PLA2G4D* (rattus organoid; Cluster 2) maintained specificity to organoids. In addition, *CACNA1D*, *MYH11*, *KCNMB1*, *CALCRL*, *IRAG1*, *CACNA1C*, *AGTR1*, *ADCY5*, *EDNRA*, *MYLK*, *ACTA2*, and *ACTG2* were classified to a tissue-specific cluster (Cluster 18), with some genes representing specific characteristics of tissues of each species (bovine: *NPPC*, feline: *EDN3*, porcine: *MYLK2*, rattus: *AVPR1A* and *PLA2G2D*).

DISCUSSION

In this study, endometrial organoids were isolated and cultured from endometria of five mammals—cows, dogs, pigs, cats, and rats—with the addition of some components, including GlutaMAX, HEPES, and Y-27632, to conventional human endometrial organoid media (Supplementary Table 9). GlutaMAX in organoid culture media can improve the maintenance and growth of organoids over extended periods (16) and Y-27632 can enhance cell survival, cell proliferation, and organoid formation (17). We maintained all endometrial organoids for at least 13 passages, demonstrating their potential for long-term storage through successful cryopreservation and regrowth (Supplementary Fig. 1). However, relatively larger lumens were formed in porcine and rattus organoids than in organoids of other species (Fig. 1B). This suggests that the medium composition used in this study might not be optimal for each species. Therefore, future research should consider either excluding certain growth factors (e.g., EGF and Noggin) or pathway inhibitors (e.g., ALK-4/5/7 inhibitor and Y-27632) from the composition or adjusting their concentrations for improvement. From a different perspective, previous research has shown that oviduct organoids from various species display distinct morphological characteristics (18), suggesting that differences in placental types and/or species-specific factors might have contributed to these observations.

Additionally, histological staining including H&E and PAS along with IHC analysis using Ki-67 for cell proliferation (14),

vimentin for stromal cells (19), and E-cadherin for glandular epithelium (20) revealed that organoids retained histological characteristics of their original uterine tissues. These findings reaffirmed that, as in previous studies, organoids could be a valuable *in vitro* model for endometrial biology and pathology (11, 12). Organoids were successfully passaged every 7 days, with organoid sizes showing variations across species. The average diameter ranked from largest to smallest as follows: rat > pig > dog > cat > cow. While organoids from pig and rat displayed distinct lumen formation, the other three species (cow, dog, and cat) exhibited spherical growth without forming a well-defined lumen. As mentioned earlier, this suggests that endometrial organoid culture medium might need to be tailored to optimize growth and structural features for each species. Additionally, Ki-67 expression was consistently higher in organoids than in original uterine tissues across all species, aligning with a previous organoid study (18) and indicating a heightened proliferative capacity within organoid culture.

We mapped trimmed raw data for transcriptome profiling based on each species' unique genetic information, identifying DEGs between organoids and tissues in each species. However, the steep slope observed in DEG patterns highlighted the limitation of biological replicates (Supplementary Fig. 2). To address this, we analyzed DEGs by dividing 10 samples into two groups (organoids: n = 5; and tissues: n = 5). Annotation of human genes reduced species-specific genetic variability, allowing for a more accurate classification of common molecular characteristics of organoids across species.

Comparing endometrial organoids to tissues, we identified a total of 707 DEGs, representing about 4.8% of the total 14,786 genes. MDS analysis of expression profiles indicated species-specific transcriptional patterns of each type of endometrial organoid and tissue distinguishable based on distance (Supplementary Fig. 3). Functional enrichment analysis of the 707 DEGs showed physiological functions of endometrial organoids compared to tissues. GO-based analysis revealed activation of tyrosine phosphorylation, extracellular matrix (ECM), and integrin binding, indicating that cell migration-related signaling pathways were more pronounced in organoids than in tissues (21). The KEGG-based analysis identified significantly enriched pathways such as the PI3K-Akt signaling pathway, ECM-receptor interaction, and focal adhesion. These pathways are actively investigated in cancer and tumor studies (22-24). These findings suggest that organoids are useful models for cancer research by mimicking the tumor microenvironment and cell-cell interactions.

Hormone metabolism (steroid biosynthesis) in organoids showed higher fold-enrichment than in tissues (Fig. 2C). Moreover, it showed the most significant value (P-value = 1.48E-07) with a high fold-enrichment in organoid-specific clusters (Cluster 7) (Supplementary Table 7), highlighting specific characteristics of each sample. Common genes identified in organoids included *SQLE*, *DHCR7*, *CYP51A1*, *EBP*, *CYP3A7*, *TM7SF2*, and *CYP24A*, all closely related to hormone metabolism in the

endometrium. Notably, *CYP24A1* can regulate vitamin D metabolism, playing a crucial role in adipocyte formation and function (25). *SULT1E1* identified specifically in bovine organoids with cotyledonary placentas can catalyze sulfation to promote estrogen inactivation, preventing excessive estrogen activation in the endometrium and reflecting the long gestation period of cows (26). *CYP1A2* specific to canine organoids with zonary placentas can metabolize carcinogens to form toxic intermediates, playing an essential role in carcinogenesis (27). Although *SRD5A2* did not meet network criteria, its expression pattern suggests that it is a specific gene in feline organoids. Porcine organoids with diffuse placentas showed specific genes such as *CYP2E1*, *CYP7A1*, and *UGT1A3* related to oxidative stress and hormone metabolism balance (28-30). Although it was challenging to verify the exact information because porcine endometrial tissues were collected from slaughterhouses, it was likely that samples were taken after multiple births, indicating potential aging. In this regard, expression levels of *CYP2E1*, *CYP7A1*, and *UGT1A3* are increased with aging (31). *HSD3B2* specific to *rattus* organoids with discoid placentas is essential for steroid hormone synthesis, playing significant roles in regulating physiological cycles, preparing for implantation, and maintaining pregnancy (32). Interestingly, although most DEGs were downregulated in organoids compared to those in tissues (Fig. 2A), genes related to hormone metabolism were predominantly upregulated. This suggests that endometrial organoids might be suitable for studying metabolism of hormones such as estrogen and progesterone in the endometrium.

Conversely, genes in the tissue-specific cluster (Cluster 18) related to vascular smooth muscle contraction were very weakly expressed in organoids, indicating that endometrial organoids might not adequately replicate complex vascular and smooth muscle contraction functions of tissues. Generally, endometrial organoids mimic epithelial cells of the endometrium, which might result in lower expression of genes related to vascular and smooth muscle contraction (13). Additionally, the enhanced PI3K-Akt signaling, ECM-receptor interaction, and focal adhesion pathways in organoids might have contributed to changes in the metabolism of vascular and smooth muscle contraction by influencing hormone synthesis and metabolism in organoids (33). This suggests that the similarity of endometrial organoids to epithelial cells of the endometrium might have resulted in stronger expression of genes related to hormone synthesis pathways in organoids compared to actual tissues, whereas genes related to vascular and smooth muscle contraction pathways are mostly downregulated due to epithelial cell characteristics of endometrial organoids.

Interest in vascular and smooth muscle contraction in the endometrium is crucial for studying menstrual cycles, endometriosis, and infertility treatments (34, 35). Therefore, developing more complex organoids is necessary. Many researchers have recognized the need for such complex organoids, leading to proposals and reports on co-culturing with other cells and gene editing of organoids (36-38). However, pure organoids may

offer advantages over actual tissues for studying characteristics such as hormone metabolism. Thus, adjusting complexity according to research focus is essential (39).

Despite classifying characteristics of endometrial organoids through integrated analysis, the limitation of sample size remains owing to the difficulty in collecting uterine tissue samples. This limitation also poses a challenge as each sample may not fully represent respective species. Hence, future studies should aim to collect samples from various time points for each species to identify expression patterns over different stages, thereby strengthening the role of organoids as flexible models representing the species. Furthermore, for improving large luminal formation observed in rats and pigs and for enhancing lifespan and functionality, culture conditions need to be refined. Improvements identified in the present study are anticipated to facilitate more in-depth analyses in subsequent organoid research.

In conclusion, we successfully isolated endometrial organoids from five mammalian species with four types of placentas and established a stable organoid model by growing organoid cultures for more than 13 passages. Subsequently, we classified unique characteristics and molecular roles of each species' endometrial organoids through integrated transcriptome profiling. This integrated analysis method compensates for the limitation of sample size and provides an innovative approach to interpreting complex characteristics of various species. Additionally, we confirmed sufficient similarity between endometrial organoids and actual tissues. We also identified the need for differentiated approaches in hormone metabolism and vascular contraction pathways. Histological and molecular characteristics of endometrial organoids for each mammalian species are described along with prospective obstacles to complete replacement of tissue models. Findings of this study mark an important starting point for building crucial data in veterinary obstetrics. They provide foundational data for future applications of organoid research in uterine disease models, regenerative medicine, and drug development.

MATERIALS AND METHODS

Ethical approval

Uterine tissues from cow and pig were obtained with permission during the slaughter process at slaughterhouses (Gyeonggi-do Animal Hygiene Testing Center, Republic of Korea). Uterine tissues from dog and cat were collected with consent for donation. Specifically, dog uterine tissue was sampled during volunteer spaying surgeries for shelter dogs, and cat uterine tissue was sampled during routine spaying procedures at local animal hospitals. For rat tissue sampling, all rat care and experiments were approved by the Institutional Animal Care and Use Committee (No. SNU-201222-4-2) of the Seoul National University Institute of Laboratory Animal Resources, and all procedures were performed following the guidelines of Seoul National University. All animal experiments were performed

following the ARRIVE guidelines (<https://arriveguidelines.org>).

Sample collection and endometrial organoid culture

Uterine tissue samples from cow (Hanwoo, 9 months old, nulliparous) and pig (N/A) were sourced from discarded tissues at slaughterhouses. For dog (mixed, 18 months old, N/A) and cat (British straight, 6 months old, nulliparous), samples were obtained during spaying procedures at local veterinary clinics. In the case of rats (Sprague-Dawley, 8 to 10 weeks old, nulliparous), anesthesia was administered using Alfaxan Multidose (Careside, Cat# 470750, Seongnam-si, Republic of Korea) and Rompun (Elanco, Cat# 90204280, Greenfield, IN, USA) to collect uterine tissue samples. Furthermore, a surgical blade was used to cut the uterus into 3-mm pieces in a 100-mm Petri dish. The diced tissue was rinsed thrice with 3 ml of phosphate buffered saline (PBS) (Gibco, Cat# 20012-027, Grand Island, NY, USA) containing 10% penicillin/streptomycin (P/S, Gibco, Cat# 15140-122). Then, the tissue was treated with 3 ml of an enzymatic dissociation solution (STEMCELL, Cat# 100-0485, Vancouver, Canada) and incubated at room temperature in a shaking incubator for 1 h. Next, 3 ml of 10% fetal bovine serum (FBS) (Gibco, Cat# 12483-020) in Dulbecco's modified Eagle medium/Nutrient Mixture F-12 (DMEM-F12) (Gibco, Cat# 12634-010) was added to deactivate the enzymatic reaction. The mixture was filtered through a 70-μm pore strainer (SPL, Cat# 93070, Pocheon-si, Republic of Korea), and the resulting solution was centrifuged at 500 × g for 5 min. The resultant pellet was rinsed with PBS, warmed to room temperature, and centrifuged again. To remove the red blood cells (RBCs), the pellet was suspended in 500 ml of RBC Lysis Solution (Invitrogen, Cat# 00-4333-57, Waltham, MA, USA) and incubated for 5 min at 4°C. Following this, centrifugation was repeated, followed by washing and centrifugation with 200 ml of 10% FBS/DMEM-F12. The pellet was then suspended in 10 μl of 10% FBS/DMEM-F12 medium. Subsequently, 90 μl of Matrigel (Corning, Cat# 356231, Glendale, AZ, USA) was added and mixed with the suspension. Furthermore, 20-μl drops of this mixture were placed on a cell culture plate (Corning, Cat# 3548) to form domes. After incubation for 20 min at 37°C with 5% CO₂, the domes were coated with 250 μl of medium. The medium was replaced every 2 or 3 days, and passages were performed every 7 days.

Management of endometrial organoids

Media composition: for the composition of the endometrial organoids culture in five mammals, we referenced the protocol established for human endometrial organoids and long-term culture as detailed by (20) and added some additional components: 20 mM HEPES (Sigma-Aldrich, Cat# H6147, St. Louis and Burlington, MA, USA), 1% GlutaMAX (Gibco, Cat# 35050-061), and 1% P/S as a final concentration. Furthermore, Y-27632 (AbMole, Cat# M1817, Houston, TX, USA) was added at a concentration of 10 μM from the initial subculture to the Passage 3 stage. The media composition is detailed in Supple-

mentary Table 9.

Passaging: we decomposed the domes using the cultured organoid media, collected them into a 1.5-ml tube, and briefly centrifuged. The medium was removed, and 200 μ l of TrypLE (Gibco, Cat# 12605-010) was added before incubating for 4 min at 37°C with 5% CO₂. Following incubation, the TrypLE reaction was halted by adding an equal volume of 10% FBS/DMEM-F12 medium. Next, the pellets were resuspended in a mixture of 10% FBS/DMEM-F12 and Matrigel in a 10:1 ratio.

Freezing: after removing the cultured organoid medium, the dome was decomposed with PBS and collected into a 1.5-ml tube. Following that, the mixture was briefly centrifuged at 500 \times g for 30 s. Then, the PBS was removed, and the pellet was resuspended in organoid freezing media CryoStor® CS10 (STEMCELL, Cat# 100-1061). The suspension was then transferred to a cryotube. The cryotube was initially frozen at -80°C for 24 h using a freezing container and subsequently transferred to a liquid nitrogen tank for storage.

Measurement of organoid diameters

Organoid diameters were determined by measuring the longest axis across each of 50 randomly selected organoids using ImageJ software (NIH, Bethesda, MD, USA) on bright-field images taken at day 7 of culture.

Formalin-fixed paraffin-embedded blocks

Uterine tissue segments of 1 cm, which were not used for organoid culture, and five organoid domes with passage numbers of 10 or higher were used for formalin fixation. For tissue fixation, the sample tissue was washed thrice with 1% P/S in PBS and fixed in 3 ml of 4% PFA. For organoid fixation, Matrigel was removed by treatment with 500 μ l of Cell Recovery Solution (Corning, Cat# 354253) for 3 min on ice before fixation. After that, each fixed sample was dehydrated using an ethanol series (70%, 95%, and 99.9%) and then embedded in paraffin wax. Sections of 3- μ m thickness were obtained, deparaffinized, rehydrated, and used for histological staining and immunostaining.

Histological staining

PAS staining was performed by oxidizing the sections in a 0.5% periodic acid solution, followed by staining with Schiff's reagent (Fisher Scientific, Cat# 50-301-27, Waltham, MA, USA) and Mayer's hematoxylin (Fisher Scientific, Cat# NC9220898). H&E staining was performed using hematoxylin (Poly Scientific, Cat# s212a Bayshore, NY, USA) and eosin (Poly Scientific, Cat# s176). The stained sections were scanned using an optical microscope.

IHC

Rehydrated tissues underwent antigen retrieval using a heat-mediated method with Tris-EDTA buffer (pH 9.0) and were pretreated with 3% H₂O₂ to block endogenous peroxidase activity. For IHC staining, primary antibodies, E-cadherin (Santa

Cruz, Cat# sc-59778, Dallas, TX, USA), vimentin (Santa Cruz, Cat# sc-373717), and Ki-67 (Invitrogen, Cat# 14-5698-82), were used. Secondary antibodies (Agilent Technologies, Cat# K400111-2 and K400311-2, Santa Clara, CA, USA) were applied, and chromogenic detection was developed using 3,3'-diaminobenzidine to produce a brown precipitate, which was visualized using optical microscopy.

RNA-seq

Ten total RNA samples were isolated from the endometrial organoids and uterine tissues of each species (cow, dog, cat, pig, and rat) using the RNeasy mini-Kit (Qiagen, Cat# 74104, Hilden, Germany) following the manufacturer's guidelines. The quantification and purity assessment of the extracted 10 total RNAs was performed using the TapeStation RNA ScreenTape (Agilent Technologies). Subsequently, total cDNA was synthesized for library construction using the TruSeq Stranded mRNA Prep Kit (Illumina, Cat# 20020594, San Diego, CA, USA), following the manufacturer's protocol. The Illumina NovaSeq 6000 (Illumina) was used to analyze the constructed libraries, performing paired-end sequencing (2 \times 100 bp). All raw RNA-seq data generated in this study were deposited in the NCBI Sequence Read Archive database under the accession number PRJNA1124246.

Data processing

To select the quality-filtering strategy, raw read data from each sample were subjected to quality checks using FastQC software v0.11.9. Based on the quality results, poor-quality reads and adaptors were trimmed using Trimmomatic software v0.39. The trimmed reads were then mapped to the reference genome (ARS-UCD1.3, GCA_002263795.3; ROS_Cfam_1.0, GCA_014441545.1; Felis_catus_9.0, GCA_000181335.4; Sus_scrofa_11.1, GCA_000003025.6; mRatBN7.2, GCA_015227675.2) from the Ensembl genome browser (https://www.ensembl.org/Bos_taurus/, https://www.ensembl.org/Canis_lupus_familiaris/, https://www.ensembl.org/Felis_catus/, https://www.ensembl.org/Sus_scrofa/, https://www.ensembl.org/Rattus_norvegicus/) using the default settings of HISAT2 v2.2.1. The raw counts corresponding to the genes of each library were calculated based on the exons of GTF v111 (Ensembl) for each species using featureCounts of the Subread package v2.0.3.

DEG analyses

All DEG analyses for the obtained raw counts were conducted using the edgeR R package v4.0.16 of Bioconductor. Normalization of the raw counts was performed using the trimmed mean of M-value (TMM) method, and dispersion parameters were estimated and applied using edgeR. First, DEGs between endometrial organoid and uterine tissue were identified for each species using a negative binomial generalized linear model. Second, DEGs between endometrial organoids and uterine tissues were identified for all combined species using human gene annotation (GRCh38 v111 GTF, overlapping

14,786 genes) using the same methods. P-values were corrected for multiple comparisons based on the Benjamini-Hochberg procedure with a false discovery rate (FDR). DEGs were determined using criteria: FDR of < 0.05 and an absolute \log_2 fold-change (FC) of ≥ 1 . MDS based on the human-annotated genes was conducted using the limma R package v3.58.1 to identify the similarities among samples.

Construction of a GCN

GCN analysis was performed using all samples' \log_2 TMM for (i) DEGs (only genes with gene symbols were used after human gene annotation) that were significant at least once in each species and (ii) DEGs that were calculated from all combined species. Significant associations between the genes were determined using the Partial Correlation Coefficient with Information Theory algorithm (40). GCN was constructed using genes with absolute co-expression correlations of ≥ 0.95 . Visualization was performed using Cytoscape v3.7.1 software, resulting in a network comprising genes (nodes) and their interactions (edges). The network did not visualize small parts consisting of fewer than 10 nodes.

Clustering analysis

Clustering analysis was conducted using the \log_2 TMM values of samples in the constructed network. After determining the optimal number of clusters, the genes were analyzed with the K-means clustering algorithm, specifying 18 clusters and 100,000 iterations, utilizing the MultiExperiment Viewer software.

Functional analyses

DEGs between endometrial organoids and uterine tissues were annotated to GO terms and Kyoto Encyclopedia of KEGG pathways using the Database for Annotation, Visualization, and Integrated Discovery (DAVID). Genes from each cluster were also annotated to KEGG pathways using DAVID. GO annotations were performed for BPs, CCs, and MFs using the DIRECT option. Treemaps of the annotated GO terms were visualized using the REVIGO tool. KEGG annotations were represented by the $-\log_{10}$ P-value and fold enrichment. All annotations adhered to the cut-offs of P-value < 0.05 and counts ≥ 3 . Annotations were conducted for *Homo sapiens*. In addition, heatmaps were generated using genes included in selected significant pathways.

AVAILABILITY OF DATA

We have submitted the RNA-seq data to the NCBI SRA with the accession number PRJNA1124246.

ACKNOWLEDGEMENTS

We appreciate all the members of the G. Jang lab for their valuable comments. Some of the figures in this paper were created with BioRender.com.

CONFLICTS OF INTEREST

The authors have no conflicting interests.

FUNDING

This study was supported financially by NRF-2021R1A5A1033157 for SRC program: 382 Comparative medicine Disease Research Center, the Research Institute of Veterinary Science, the BK21 Four for Future Veterinary Medicine Leading Education and Research Center, SNU#550-20240037 and the National Research Foundation of Korea (NRF-550-20240031).

REFERENCES

1. Zhang J, Wang C, Jia C et al (2022) The role of circular RNAs in the physiology and pathology of the mammalian ovary. *Int J Mol Sci* 23, 15204
2. Kordowitzki P, Kranc W, Bryl R et al (2020) The relevance of aquaporins for the physiology, pathology, and aging of the female reproductive system in mammals. *Cells* 9, 2570
3. Garcia-Alonso L, Handfield LF, Roberts K et al (2021) Mapping the temporal and spatial dynamics of the human endometrium *in vivo* and *in vitro*. *Nat Genet* 53, 1698-1711
4. Emera D, Romero R and Wagner G (2012) The evolution of menstruation: a new model for genetic assimilation: explaining molecular origins of maternal responses to fetal invasiveness. *BioEssays* 34, 26-35
5. Ross JW, Ashworth MD, Mathew D et al (2010) Activation of the transcription factor, nuclear factor kappa-B, during the estrous cycle and early pregnancy in the pig. *Reprod Biol Endocrinol* 8, 39
6. Chadchan SB, Popli P, Liao Z et al (2024) A GREB1-steroid receptor feedforward mechanism governs differential GREB1 action in endometrial function and endometriosis. *Nat Commun* 15, 1947
7. Carvalho C, Gaspar A, Knight A et al (2019) Ethical and scientific pitfalls concerning laboratory research with non-human primates, and possible solutions. *Animals* 9, 12
8. Malvezzi H, Marengo EB, Podgaec S et al (2020) Endometriosis: current challenges in modeling a multifactorial disease of unknown etiology. *J Transl Med* 18, 311
9. Richter M, Piwocka O, Musielak M et al (2021) From donor to the lab: a fascinating journey of primary cell lines. *Front Cell Dev Biol* 9, 711381
10. Tang XY, Wu S, Wang D et al (2022) Human organoids in basic research and clinical applications. *Signal Transduct Target Ther* 7, 168
11. Silva-Pedrosa R, Salgado AJ and Ferreira PE (2023) Revolutionizing disease modeling: the emergence of organoids in cellular systems. *Cells* 12, 930
12. Li Y, Tang P, Cai S et al (2020) Organoid based personalized medicine: from bench to bedside. *Cell Regen* 9, 21
13. Gu ZY, Jia SZ, Liu S et al (2020) Endometrial organoids: a new model for the research of endometrial-related diseases. *Biol Reprod* 103, 918-926
14. Boretto M, Cox B, Noben M et al (2017) Development of organoids from mouse and human endometrium showing

- endometrial epithelium physiology and long-term expandability. *Development* 144, 1775-1786
- 15. Furukawa S, Kuroda Y and Sugiyama A (2014) A comparison of the histological structure of the placenta in experimental animals. *J Toxicol Pathol* 27, 11-18
 - 16. Wang R, Mao Y, Wang W et al (2022) Systematic evaluation of colorectal cancer organoid system by single-cell RNA-Seq analysis. *Genome Biol* 23, 106
 - 17. Li Z, Han S, Wang X et al (2015) Rho kinase inhibitor Y-27632 promotes the differentiation of human bone marrow mesenchymal stem cells into keratinocyte-like cells in xeno-free conditioned medium. *Stem Cell Res Ther* 6, 17
 - 18. Lawson EF, Ghosh A, Blanch V et al (2023) Establishment and characterization of oviductal organoids from farm and companion animals. *Biol Reprod* 108, 854-865
 - 19. Wiwatpanit T, Murphy AR, Lu Z et al (2020) Scaffold-free endometrial organoids respond to excess androgens associated with polycystic ovarian syndrome. *J Clin Endocrinol Metab* 105, 769-780
 - 20. Turco MY, Gardner L, Hughes J et al (2017) Long-term, hormone-responsive organoid cultures of human endometrium in a chemically defined medium. *Nat Cell Biol* 19, 568-577
 - 21. Bao Y, Wang L, Shi L et al (2019) Transcriptome profiling revealed multiple genes and ECM-receptor interaction pathways that may be associated with breast cancer. *Cell Mol Biol Lett* 24, 38
 - 22. Zhang Z, Li J, Jiao S et al (2022) Functional and clinical characteristics of focal adhesion kinases in cancer progression. *Front Cell Dev Biol* 10, 1040311
 - 23. Tan X, Kong D, Tao Z et al (2024) Simultaneous inhibition of FAK and ROS1 synergistically repressed triple-negative breast cancer by upregulating p53 signalling. *Biomark Res* 12, 13
 - 24. Bhattacharya A, Alam K, Roy NS et al (2023) Exploring the interaction between extracellular matrix components in a 3D organoid disease model to replicate the pathophysiology of breast cancer. *J Exp Clin Cancer Res* 42, 343
 - 25. Jang H, Choi Y, Yoo I et al (2017) Vitamin D-metabolic enzymes and related molecules: expression at the maternal-conceptus interface and the role of vitamin D in endometrial gene expression in pigs. *PLoS One* 12, e0187221
 - 26. Yi M, Negishi M and Lee SJ (2021) Estrogen sulfotransferase (SULT1E1): its molecular regulation, polymorphisms, and clinical perspectives. *J Pers Med* 11, 194
 - 27. Wang H, Zhang Z, Han S et al (2012) CYP1A2 rs762551 polymorphism contributes to cancer susceptibility: a meta-analysis from 19 case-control studies. *BMC Cancer* 12, 528
 - 28. Schattenberg JM and Czaja MJ (2014) Regulation of the effects of CYP2E1-induced oxidative stress by JNK signaling. *Redox Biol* 3, 7-15
 - 29. Jarrar Y and Lee SJ (2021) The functionality of UDP-glucuronosyltransferase genetic variants and their association with drug responses and human diseases. *J Pers Med* 11, 554
 - 30. Lammel Lindemann JA, Angajala A, Engler DA et al (2014) Thyroid hormone induction of human cholesterol 7 alpha-hydroxylase (Cyp7a1) *in vitro*. *Mol Cell Endocrinol* 388, 32-40
 - 31. Xu SF, Hu AL, Xie L et al (2019) Age-associated changes of cytochrome P450 and related phase-2 gene/proteins in livers of rats. *PeerJ* 7, e7429
 - 32. Wang L, Salavaggione E, Pelleymounter L et al (2007) Human 3β-hydroxysteroid dehydrogenase types 1 and 2: gene sequence variation and functional genomics. *J Steroid Biochem Mol Biol* 107, 88-99
 - 33. Cullen AE, Centner AM, Deitado R et al (2023) AKT mediates adiponectin-dependent regulation of VSMC phenotype. *Cells* 12, 2493
 - 34. Watters M, Martínez-Aguilar R and Maybin JA (2022) The menstrual endometrium: from physiology to future treatments. *Front Reprod Health* 3, 794352
 - 35. Salamonsen LA, Hutchison JC, Gargett CE (2021) Cyclical endometrial repair and regeneration. *Development* 148, dev199577
 - 36. Cheung VC, Peng CY, Marinić M et al (2021) Pluripotent stem cell-derived endometrial stromal fibroblasts in a cyclic, hormone-responsive, coculture model of human decidua. *Cell Rep* 35, 109138
 - 37. Lou L, Kong S, Sun Y et al (2022) Human endometrial organoids: recent research progress and potential applications. *Front Cell Dev Biol* 10, 844623
 - 38. Naderi-Meshkin H, Cornelius VA, Eleftheriadou M et al (2023) Vascular organoids: unveiling advantages, applications, challenges, and disease modelling strategies. *Stem Cell Res Ther* 14, 292
 - 39. Kim J, Koo BK and Knoblich JA (2020) Human organoids: model systems for human biology and medicine. *Nat Rev Mol Cell Biol* 21, 571-584
 - 40. Reverter A and Chan EKF (2008) Combining partial correlation and an information theory approach to the reversed engineering of gene co-expression networks. *Bioinformatics* 24, 2491-2497